ISSN 0957-4484

NANOTECHNOLOGY

VOLUME 18 NUMBER 45 14 NOVEMBER 2007

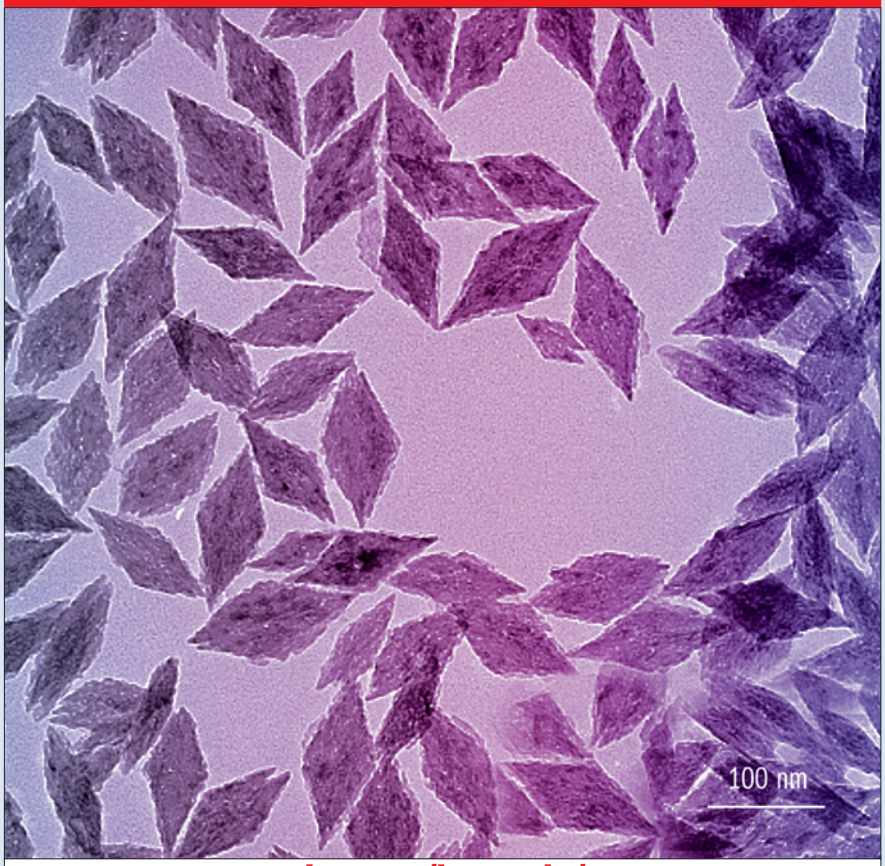

www.iop.org/journals/nano

Featured article:

An ionic liquid based synthesis method for uniform luminescent lanthanide fluoride nanoparticles

Nuria O Nuñez and Manuel Ocaña

IOP Publishing

IOP PUBLISHING NANOTECHNOLOGY
Nanotechnology **18** (2007) 455703 (9pp) doi:10.1088/0957-4484/18/45/455703

Properties of halloysite nanotube–epoxy resin hybrids and the interfacial reactions in the systems

Mingxian Liu, Baochun Guo, Mingliang Du, Xiaojia Cai and Demin Jia

Department of Polymer Materials and Engineering, South China University of Technology, Guangzhou 510640, People's Republic of China

E-mail: psbcguo@scut.edu.cn

Received 10 June 2007, in final form 27 August 2007
Published 10 October 2007
Online at stacks.iop.org/Nano/18/455703

Abstract
A naturally occurred microtubullar silicate, halloysite nanotubes (HNTs), was co-cured with epoxy/cyanate ester resin to form organic–inorganic hybrids. The coefficient of thermal expansion (CTE) of the hybrids with low HNT concentration was found to be substantially lower than that of the plain cured resin. The moduli of the hybrids in the glassy state and rubbery state were significantly higher than those for the plain cured resin. The dispersion of HNTs in the resin matrix was very uniform as revealed by the transmission electron microscopy (TEM) results. The interfacial reactions between the HNTs and cyanate ester (CE) were revealed by the results of Fourier transform infrared spectroscopy (FTIR) and x-ray photoelectron spectroscopy (XPS). The substantially increased properties of the hybrids were attributed to the covalent bonding between the nanotubes and the matrix.

(Some figures in this article are in colour only in the electronic version)

1. Introduction

Epoxy resins are well established as thermosetting matrices for printed circuit boards (PCB) in the electronics industry [1–5]. For such applications, the high dimensional stability (low coefficient of thermal expansion (CTE)) of the resin is crucial to the fabrication of a highly integrated PCB. To lower the CTE value of the resin, incorporating inorganics such as silica into the matrix is effective and has been widely reported [6–8]. Overloading the inorganics to epoxy resin ratio usually leads to the reduced mechanical properties of the composites and high viscosity of the epoxy resin at melting condition [9, 10]. Generally, relatively lower inorganics content in the resin is desired for the comprehensive properties and good processability of the composites. Because of the balance between properties and cost, the trend of application of nanoparticle-filled epoxy resin in the electronics packaging area highlights the need to develop a simple preparation method and explore naturally occurring nanoparticles with relative low filler loading to enhance the epoxy resin properties.

Halloysite nanotubes (HNTs) are a kind of naturally deposited aluminosilicate ($Al_2Si_2O_5(OH)_4.nH_2O$), chemically similar to kaolin, which have a predominantly hollow tubular structure in the submicrometer range with a high aspect ratio [11]. The length of HNTs varies in the range of 1–15 μm. HNTs have an inner diameter of 10–30 nm and an outer diameter of 50–70 nm, depending on the deposits. The zeta-potential behavior of HNTs is mostly negative at pH 6–7 due to the surface potential of SiO_2 with a small contribution from the positive Al_2O_3 inner surface [12]. The chemical properties of the HNTs' outermost surface are similar to the properties of SiO_2, while the properties of the inner cylinder core could be associated with those of Al_2O_3 [13]. Recently, HNTs are reported as a new type of additive for polymers such as polypropylene [14, 15] and polyvinyl alcohol [16], and increased mechanical and thermal properties of the composites were found. Comparing with other nanosized inorganic fillers, naturally occurring HNTs are easily available and much cheaper. More importantly, the unique crystal structure of HNTs, such as rod-like geometry and low hydroxyl density

on the surface, makes them readily dispersed in a polymer matrix. In the present work, HNTs were incorporated in a cyanate ester cured epoxy resin to lower the CTE value and increase the mechanical properties of the epoxy resin. Cyanate ester was selected as the hardener as it can co-cure with epoxy resin and was reported to be reactive towards the silanols of polyhedral oligomeric silsesquioxane (POSS) [17]. The abundant aluminols located in the inner side and edges of the HNTs are expected to react with cyanate ester in the hybrids. The CTE and mechanical properties of the epoxy/HNT hybrids were evaluated. The interfacial reactions between HNTs and the matrix were examined in detail.

2. Experimental details

2.1. Materials

The epoxy resin used was a liquid diglycidyl ether of bisphenol A (GELR-128, epoxy equivalent of 184–190 g/eq, Grace THW., Taiwan). The hardener, bisphenol A dicyanate ester (AroCy B-10), was purchased from Ciba Specialty Chemical Corp. The HNTs were mined from Yichang, Hubei, China. The density of the HNTs was 2.6 g cm^{-3}. The elemental composition by x-ray fluorescence (XRF) was determined as follows (wt%): SiO_2, 54.29; Al_2O_3, 44.51; Fe_2O_3, 0.63; TiO_2, 0.006. The chemical structures of the black epoxy resin and the hardener are represented as follows:

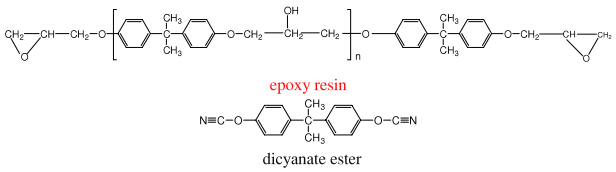

2.2. Characterization of HNTs

The HNTs were purified according to the method in [13, 18]. The Brunauer–Emmett–Teller (BET) surface area and pore structure of purified HNTs were investigated using the nitrogen adsorption method with a Micromeretics ASAP 2020. Prior to the determination of an adsorption–desorption isotherm the sample was degassed to remove the physisorbed species from the surface of the HNTs. The sample was degassed to 200 μmHg with an evacuation rate 5 mmHg s^{-1} and a heating procedure with a heating rate 10 °C min^{-1} to 90 °C. Then the sample was heated to 200 °C with a heating rate 10 °C min^{-1} and held at 200 °C and 100 mmHg for 3 h. The specific surface area was calculated by applying the BET method to the relative pressure (P/P^0) range of the isotherms between 0.05 and 0.2, taking a value of 0.162 nm^2 for the cross section of the adsorbed nitrogen molecular at 77 K. The pore-size distributions were computed by applying the Barrett–Joyner–Halenda (BJH) method. Particle size distribution of purified HNTs in water solution was conducted with a Beckman Coulter LS13 320. The following fluid was water. The morphology of the purified HNTs was observed with a LEO1530 VP SEM machine and a Philips Tecnai 12 TEM.

2.3. Preparation of the epoxy/HNT hybrids

The crude HNTs were dispersed in epoxy resin at 70 °C under stirring for 60 min and then degassed. The hardener was added and stirred for 10 min to ensure good mixing of this component. The resulting mixture was degassed for 30 min and poured into steel molds with Teflon coating. The weight ratio of epoxy resin/hardener was 100/40. The samples were cured according to the curing schedule of 150 °C/2 h + 180 °C/1 h + 200 °C/2 h. The samples were cooled to room temperature over 8 h. The concentration of HNTs in the final hybrid is variable. Generally, a higher HNT loading leads to higher viscosity and reduced processability. As a consequence, in the present work, the concentration of HNTs is not higher than 12 wt% to facilitate the degassing and casting procedures.

2.4. Characterization of the epoxy/HNT hybrids and the model compound

Coefficient of thermal expansion (CTE). CTE of the samples was measured with a NETZSCH DIL 402 PC at a heating rate of 10 °C min^{-1} from room temperature to 160 °C. The thermal expansion increases with temperature and the CTE values were calculated from the slope.

Dynamic mechanical analysis (DMA). Dynamic mechanical analysis was conducted with a NETZSCH Instruments DMA 242 at an oscillation frequency and heating rate of 1.0 Hz and 5 °C min^{-1}, respectively. The three-point bending mode was selected and the experiments were conducted under nitrogen purging.

Transmission electron microscopy (TEM). Ultrathin sections (200 nm) of the samples were cut using an ultramicrotome (EM ULTRACUT UC, Leica) and the sections were supported by holey carbon film on Cu grids. TEM analysis of the hybrids was carried out with a Philips Tecnai 12 transmission electron microscopy.

In situ FTIR. The epoxy/cyanate ester resin containing 4 wt% HNTs was used for the *in situ* FTIR experiment. The test was performed with the MAGNA-IR760 (Nicolet Co., USA) equipped heating furnace with the heating rate 5 °C min^{-1} from room temperature to 230 °C. Thirty-two consecutive scans were taken and their average was stored. Spectra were taken from 4000 to 400 cm^{-1}.

X-ray photoelectron spectroscopy (XPS). The model compound containing 5 g cyanate ester and 5 g HNTs was prepared by vigorously stirring. The model compound was treated at 180 °C/1 h and 200 °C/2 h. The FTIR spectra of the model compound before and after the thermal treatment were recorded by a Bruker Vector 33 spectrometer. XPS spectra of the model compound before and after the thermal treatment were recorded by a Kratos Axis Ultra^{DLD} with an

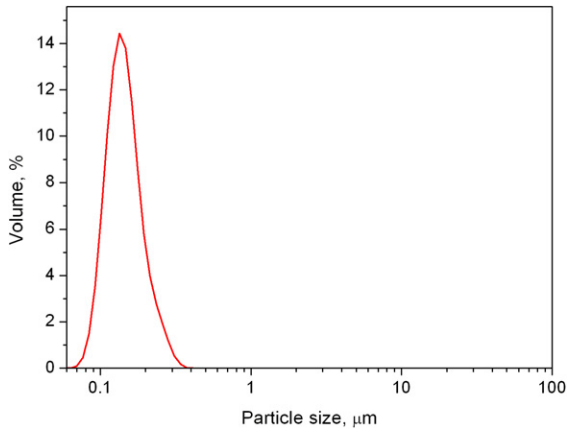

Figure 1. Particle size and distribution of HNTs in aqueous solution.

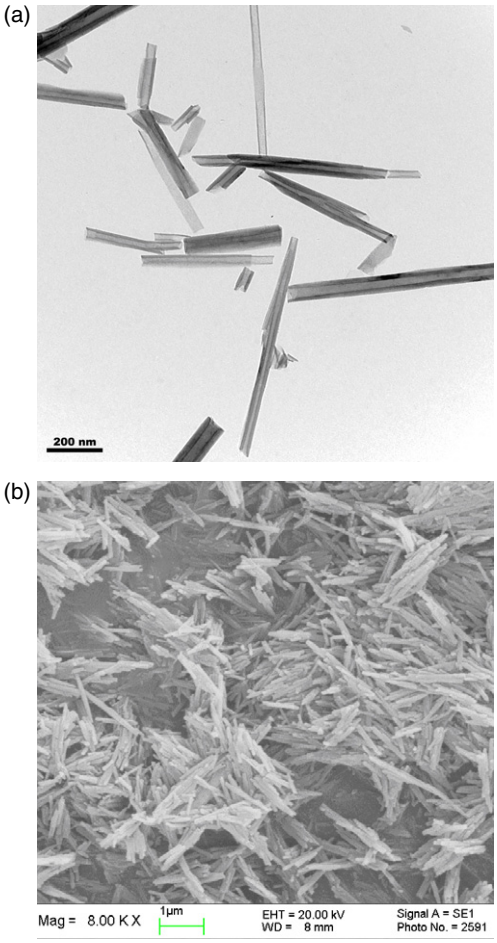

Figure 2. Morphology of the HNTs. (a) TEM photo; (b) SEM photo.

aluminum (mono) Kα source (1486.6 ev). The Al Kα source was operated at 15 kV and 10 mA. The samples were mounted onto a holder with double-sided conductive adhesive tape and placed in a vacuum of 10^{-9} Torr. The analyzed sample area was approximately 0.7 mm $\times$ 0.3 mm. For all the samples, a low-resolution survey run (0–1100 eV, pass energy = 160 eV) and a high-resolution survey (pass energy = 40 eV) were performed at spectral regions relating to nitrogen, silicon

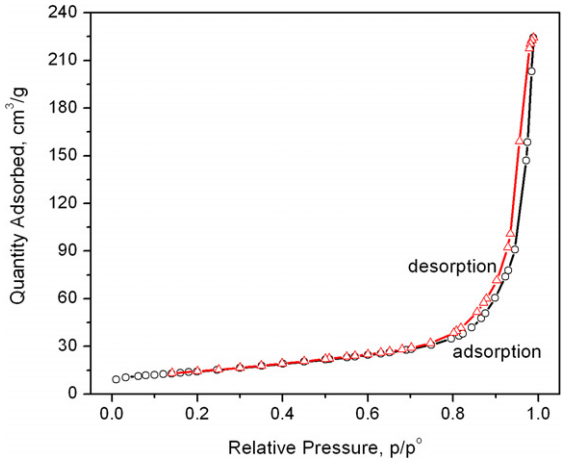

Figure 3. Nitrogen adsorption–adsorption isotherms of HNTs.

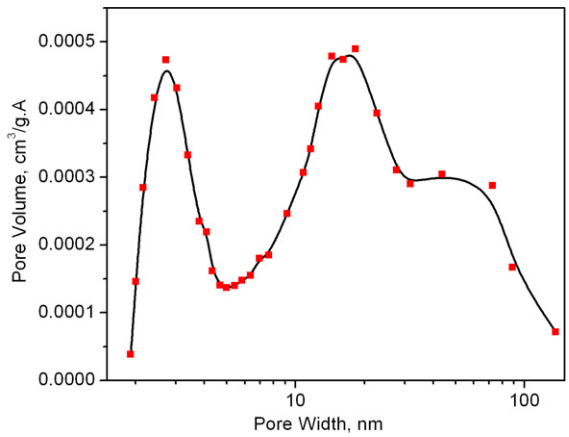

Figure 4. BJH pore size distribution of HNTs.

and aluminum. The spectra of the high-resolution survey of the three elements were deconvoluted using XPS PEAK 4.1 software into several peaks to compare the variation before and after treatment.

3. Results and discussion

3.1. Characteristics of HNTs

Figure 1 shows the particle size and distribution of HNTs in a 5 wt% aqueous solution. The mean particle size of HNTs is 0.143 μm and their size ranges from 50 to 400 nm. It can be seen from figure 2 that the HNTs are tubular with 300 nm–1.5 μm in length, 50–100 nm in outer diameter and 10–30 nm in inner diameter. The surface area analysis was carried out on HNTs by the BET method. The specific surface area is determined as 50.4 $m^2\ g^{-1}$. The nitrogen sorption isotherms of the HNTs are depicted in figure 3, showing typical II adsorption behavior [19]. In the low-pressure region ($P/P^o < 0.8$), the adsorption isotherms are relatively flat, while in the high relative pressure region ($P/P^o > 0.8$), the isotherms increase rapidly. The BJH pore size distribution curve of the HNTs is shown in figure 4. The pores range from 2 to 120 nm, which indicates that mesopores and macropores coexist on the

Table 1. CTE values of different hybrids in two different temperature ranges.

Samples wt% (vol%)		CTE, 25–100 °C (ppm °C^{-1})	Decrease (%)	CTE, 100–160 °C (ppm °C^{-1})	Decrease (%)
Neat resin		51.26	—	77.26	—
HNTs	4.0 (1.97)[a]	48.68	5.0	70.06	9.3
	8.0 (4.03)[a]	46.35	9.6	68.59	11.2
	12.0 (6.17)[a]	41.19	19.6	60.40	21.8
Silica	20.0 (10.55)[b]		Decrease 19.4% (below T_g)		
Modified ATT	13.7 (7.47)[c]		Decrease 25.0% (below T_g)		
MMT	15.0 (8.58)[d]		Decrease 27.0% (below T_g)		

[a] Calculated according to the densities of epoxy and HNTs of 1.25 and 2.59, respectively;
[b] Calculated according to the densities of epoxy and nanosized silica of 1.25 and 2.65, respectively;
[c] According to [20];
[d] Calculated according to the densities of epoxy and nanosized silica of 1.25 and 2.35, respectively.

HNTs. The peaks around 20, 50 and 3 nm are attributed to the lumens of the nanotubes, pores among the tubes and surface defects, respectively.

3.2. CTE of epoxy/HNT hybrids

Incorporation of HNTs into the epoxy resin leads to increased dimensional stability of the hybrids. The CTE values are summarized in table 1. It is shown that the CTE of the hybrids decreases with HNT content. The tendency is more obvious at relatively high temperature ranges. The CTE (25–100 °C) for the hybrids with 12 wt% HNTs is determined as 41.2 ppm °C^{-1}, which is 19.6% lower than that of the neat epoxy resin. It indicates that the HNTs are competitive with the performance of epoxy resins containing other nanosized inorganics reported in the literature [7, 21, 22]. For examples, 20 wt% nanosilica led to a 19.4% decrease in CTE of epoxy resin [7]. Incorporating 13.7 wt% of 4,4′-methylenebis(phenyl isocyanate) modified attapulgite (ATT) into epoxy resin decreased the CTE by 25% [20]. Epoxy resins showed a decrease in linear CTE of 27% for the addition of 15 wt% montmorillonite (MMT) [21]. The remarkable dimensional stability of epoxy resin/HNT hybrids may be correlated with the aluminosilicate nature of HNTs and the interfacial interactions between HNTs and matrix, which are substantiated in the results below. The interfacial interaction between the inorganics and the polymer matrix is critical to the lower CTE of the polymer containing inorganics, as the inorganics may restrict the relaxation mobility of the polymer chain segment at the polymer/inorganic interface, especially at the higher temperatures [22]. Owing to the ease of processing and lack of need of any chemical modification, the HNTs may be an excellent candidate for epoxy resin used in the electronics industry.

3.3. Viscoelastic properties of epoxy/HNTs hybrids

Generally, incorporating inorganics into a polymer matrix leads to an increased modulus of the polymer composites. HNTs were a kind of inorganic material and were found to be effective in reinforcing the thermoplastic [14, 15]. Due to the polar nature of the HNTs, they may have better compatibility with the polar epoxy resin and be expected to have good reinforcability for the epoxy resin. The dynamic modulus spectra are shown in figure 5. Table 2 summarizes the value

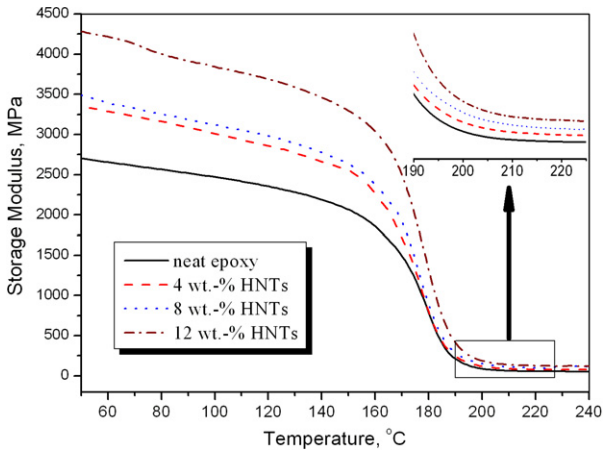

Figure 5. Storage modulus spectra of the epoxy/HNTs hybrids.

Table 2. Storage moduli of epoxy/HNTs hybrids in glassy and rubbery states.

Samples (wt%)	E′ at 50 °C (MPa)	Increase (%)	E′ at 210 °C (MPa)	Increase (%)
Neat resin	2701	—	62.8	—
4.0	3354	24.2	88.1	40.3
8.0	3491	29.2	109.7	74.7
12.0	4283	58.6	139.2	121.7

of the storage modulus at 50 and 210 °C. From figure 5 and table 2, it can be seen that the storage modulus increases with the loading of HNTs. The storage modulus of the hybrid with 12 wt% HNTs is 58.6% higher at 50 °C and 121.7% higher at 210 °C than that of the neat epoxy. Since HNTs are inorganic rigid silicate nanotubes with high aspect ratio and the interfacial reactions may take place between HNTs and the matrix, the hybrids show higher moduli at the glassy state and rubbery state. The effective reinforcing effect of HNTs on other polymers has also been illustrated [14, 15, 23, 24].

3.4. Morphology of epoxy/HNT hybrids

Figure 6 shows the TEM photos of the epoxy/HNT hybrids. It can be seen that the HNTs are dispersed in the epoxy resin very uniformly. The individually separated HNTs are found in all the samples although aggregated HNTs coexisted in the sample

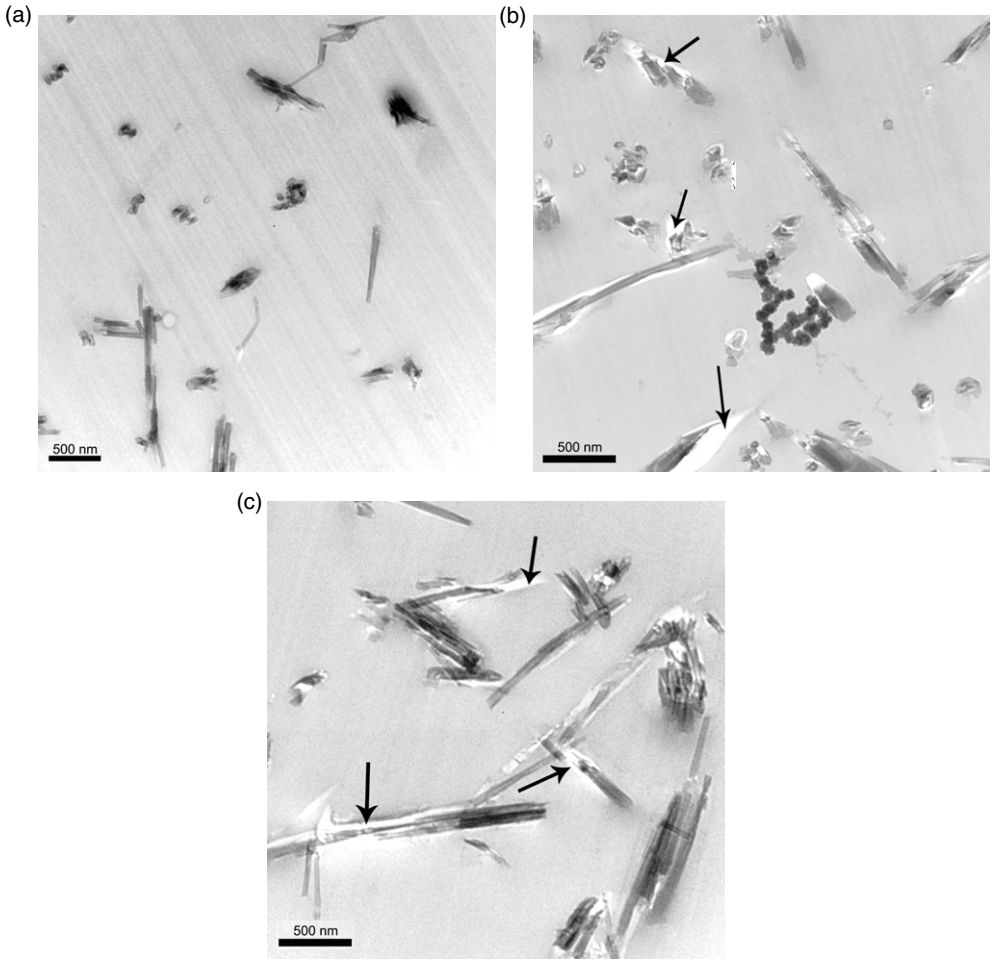

Figure 6. TEM photos of epoxy/HNT hybrids (black arrows represent the microcracks) (a) 4% HNTs; (b) 8% HNTs; (c) 12% HNTs.

with relatively higher HNT loading (12 wt%). In figures 6(b) and (c), interfacial cracking between the HNTs and the matrix was observed. The cracks appeared during the observation of the morphology of the hybrids under the high accelerating voltage used in the microscopy. Macroscopically, cracks are an indication of bad interfacial bonding. The nanoscale cracks observed in the TEM experiment, in contrast, may be attributed to the good interfacial bonding in the hybrids. The organic matrix has much higher shrinkage compared with HNTs. As a consequence, the strong interfacial bonding between the matrix and HNTs leads to cracking when the thin film is exposed to an electron beam.

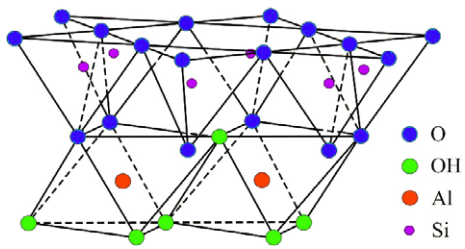

Scheme 1. Crystalline structure of HNTs.

3.5. Interfacial reactions in the hybrid systems

In order to verify the interfacial reactions between HNTs and the matrix, FTIR and XPS experiments were conducted on the hybrids and the model compounds. The curing mechanisms concerning the epoxy/cyanate ester hybrid resins were well documented [25–28]. As the authors attempt to disclose the possible interfacial reactions and hydroxyl is the only reactive group on the HNTs, only the absorptions concerning the aluminol or silanol groups and their derivatives are discussed below. HNTs have a chemical composition similar to kaolinite, which is a dioctahedral 1:1 layered aluminosilicate, consisting of two different interlayer surfaces. In the kaolinite layer, one side of the lamella is made of a Gibbsite-type layer with aluminum atoms coordinated octahedrally by oxygen atoms and hydroxyl groups (shown in scheme 1). The other side of the lamella is made of a silica-type layer in which the silicon atoms are tetrahedrally coordinated by oxygen atoms. Consequently, one side of the lamella (that of the aluminum atoms) shows hydroxyl groups, while the other side (that of the silicon atoms) has oxygen atoms [29, 30]. HNTs differ from kaolinite in that the surfaces are curved or rolled due to the misfit of the octahedral Gibbsite-like sheets and the siloxane sheets [31]. Therefore, the reactive

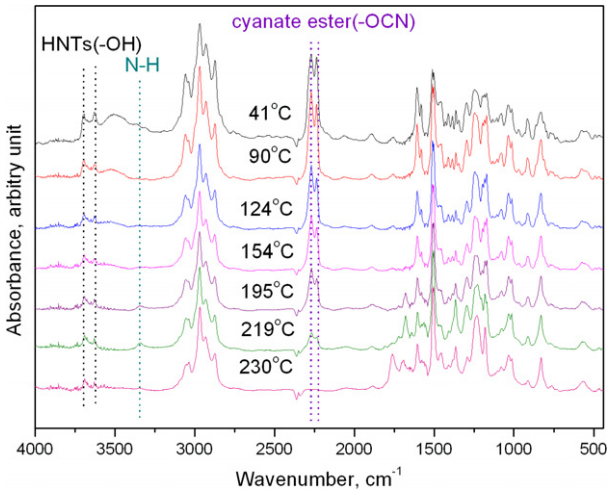

Figure 7. *In situ* FTIR spectra evolution of the epoxy/HNT hybrid system.

groups on the HNTs are predominantly aluminols which are located on the inner side or at the ends of the tubes. In addition, a few silanols located at the edges of the HNTs and surface defects should also be considered. As the epoxy groups and the hydroxyl groups of epoxy resin are inert towards the aluminols and silanols under the curing condition, the interfacial reactions between HNTs and the matrix are mainly the interactions between aluminols and silanols and the cyanate ester. The evolution of the FTIR spectrum of the hybrid containing 4 wt% HNTs during curing is presented in figure 7. The absorptions around 3620 and 3695 cm^{-1} are attributed to Al_2OH stretching [30–34], which decreases consistently and eventually becomes almost indiscernible at 230 °C. Meanwhile, a new absorption around 3343 cm^{-1}, characterizing the presence of vibrating N–H, appears. The new absorption originates from the vibrating N–H in the iminocarbonate, which is the addition product of aluminol and cyanate ester. The formation of the iminocarbonate consisting of an aluminol moiety is shown in scheme 2. Pittman *et al* [17] also reported that the hydroxyl (silanols) groups of trisilanolphenyl-POSS were reactive to the cyanate ester.

In order to further confirm the above reaction, the model compound consisting of cyanate ester and HNTs was prepared and treated at high temperature. Figure 8 shows the FTIR spectra before and after the thermal treatment. Also, the absorption around 3393 cm^{-1}, which is attributed to the vibrating N–H, is observed in the treated sample. The absorptions around 3697 and 3624 cm^{-1} are attributed to the vibration of the aluminols of the HNTs. Noticeably, the intensity ratio of $I_{3697\ cm^{-1}}/I_{2968\ cm^{-1}}$ and the $I_{3624\ cm^{-1}}/I_{2968\ cm^{-1}}$ decrease considerably, in which $I_{2968\ cm^{-1}}$ is the intensity of the C–H vibration of the internal reference peak of $-CH_3$ of the polymer. It is therefore concluded that the aluminols may react with the cyanate ester to form iminocarbonates at high temperature.

XPS is convenient in detecting binding energy variation of the elements under different chemical circumstances. In the present work, it was employed to verify the interfacial reactions. Low-resolution XPS spectra of the CE/HNT model mixture before and after thermal treatment are shown in

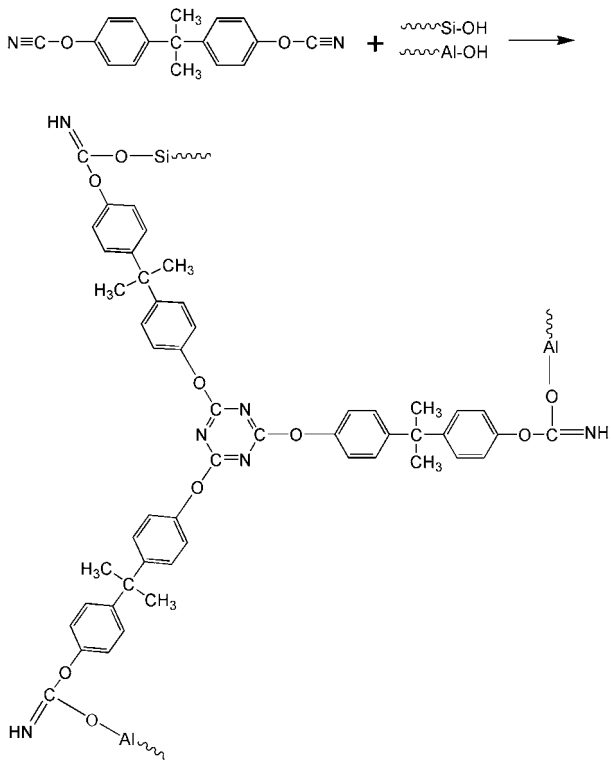

Scheme 2. Mechanism of the reaction between the hydroxyl groups and cyanate ester.

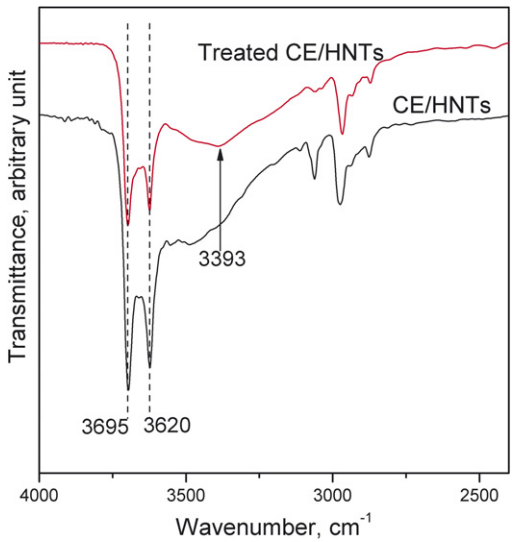

Figure 8. FTIR spectra of the model compound before and after thermal treatment.

figure 9. The figure shows the characteristic elements for the compound, including carbon, nitrogen, oxygen, silicon and aluminum. After the thermal treatment, the detected relative concentrations of silicon and aluminum are substantially lower than those for the original sample. This result may be due to the fact that the surface of the HNTs is effectively wrapped by the polymerized cyanate ester after thermal treatment. Ideally, the HNTs' surface may be wrapped completely and no silicon and

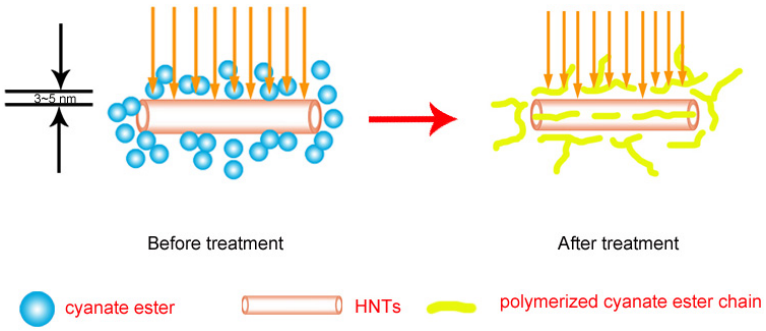

Scheme 3. Spatial arrangements of the cyanate ester/HNT model compound before and after thermal treatment.

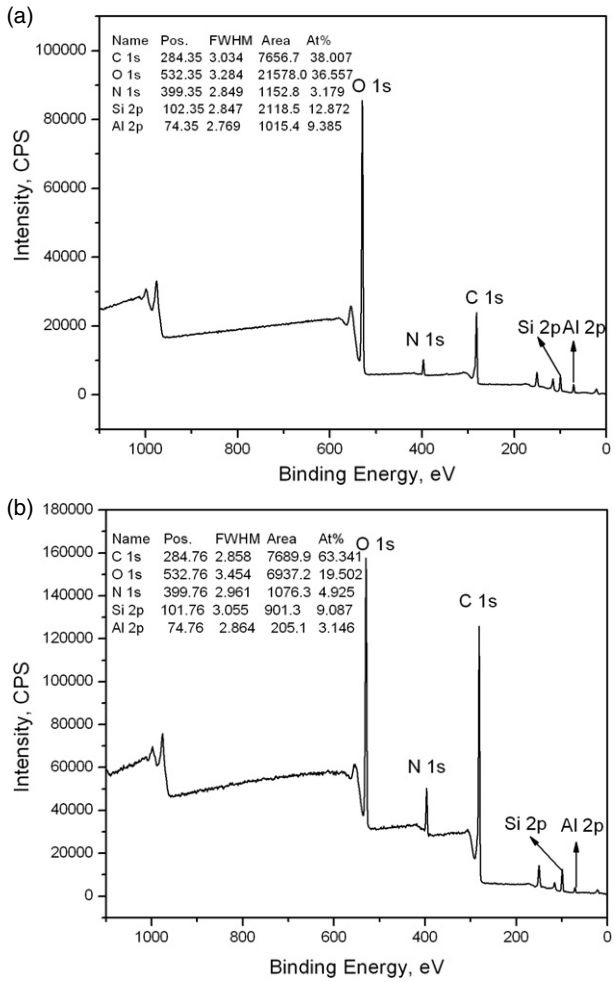

Figure 9. Low-resolution XPS survey of the model compound before (a) and after (b) thermal treatment.

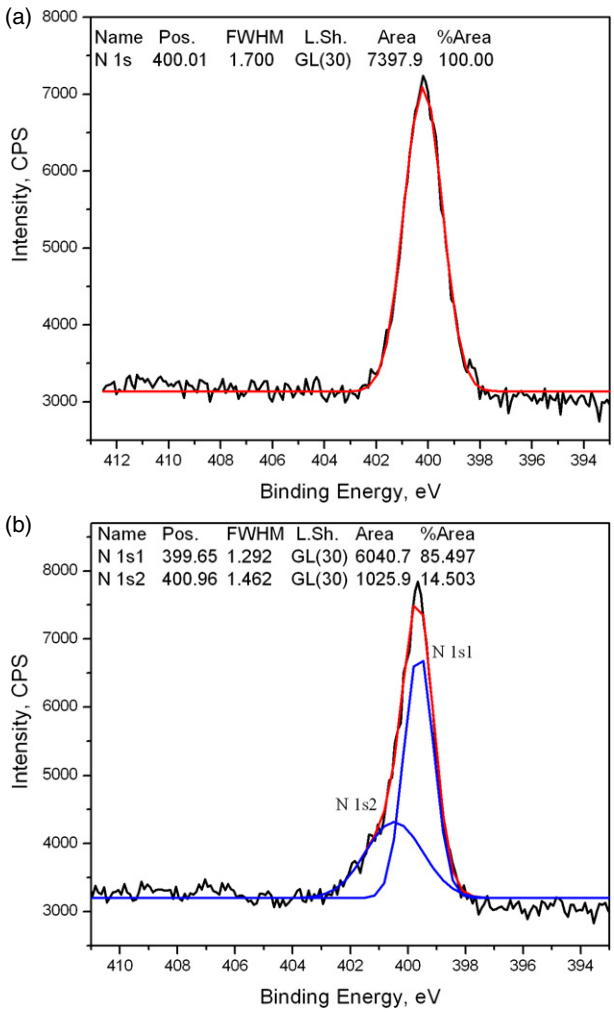

Figure 10. High-resolution XPS spectra of nitrogen for the model compound before (a) and after (b) thermal treatment.

aluminum elements could be detected by XPS in view of the typical sampling depth of 3–5 nm. However, the reactions do not deplete all of the hydroxyl groups of the HNTs, as indicated by the above-mentioned FTIR results. Consequently, the HNTs are partially wrapped after thermal treatment. As a result, the detected silicon and aluminum concentrations are remarkably lower than those for the original sample. The wrapped state of the model compound is shown in scheme 3.

To get more detailed information, a high-resolution XPS survey of nitrogen, silicon and aluminum in the two samples was performed and the results were shown in figures 10–12, respectively. The spectra of the nitrogen, silicon and aluminum were deconvoluted using XPS PEAK 4.1 software into two peaks, although it was unsuccessful for the aluminum spectrum, possibly due to the similar binding energy for

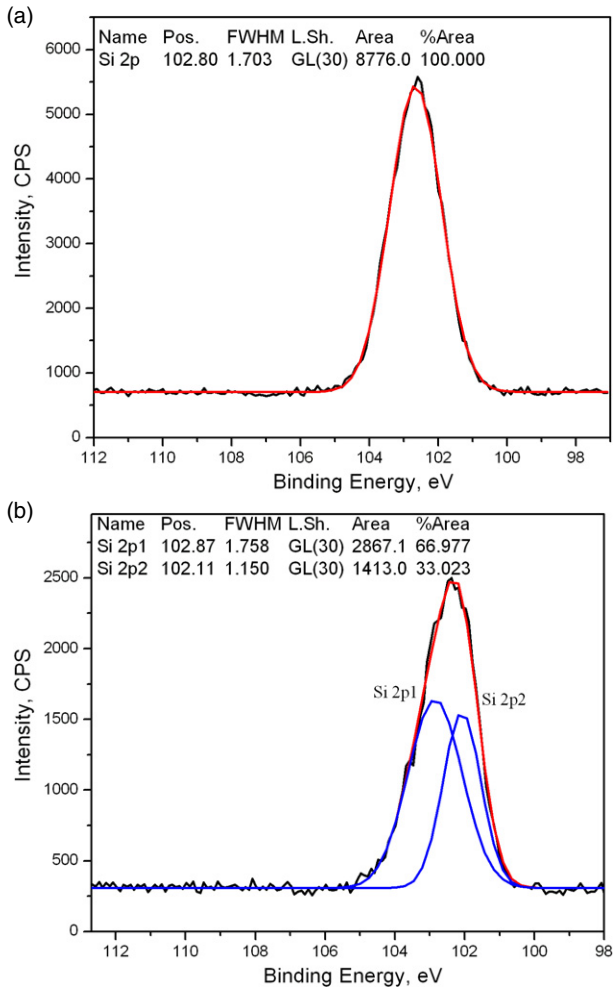

Figure 11. High-resolution XPS spectra of silicon for the model compound before (a) and after (b) thermal treatment.

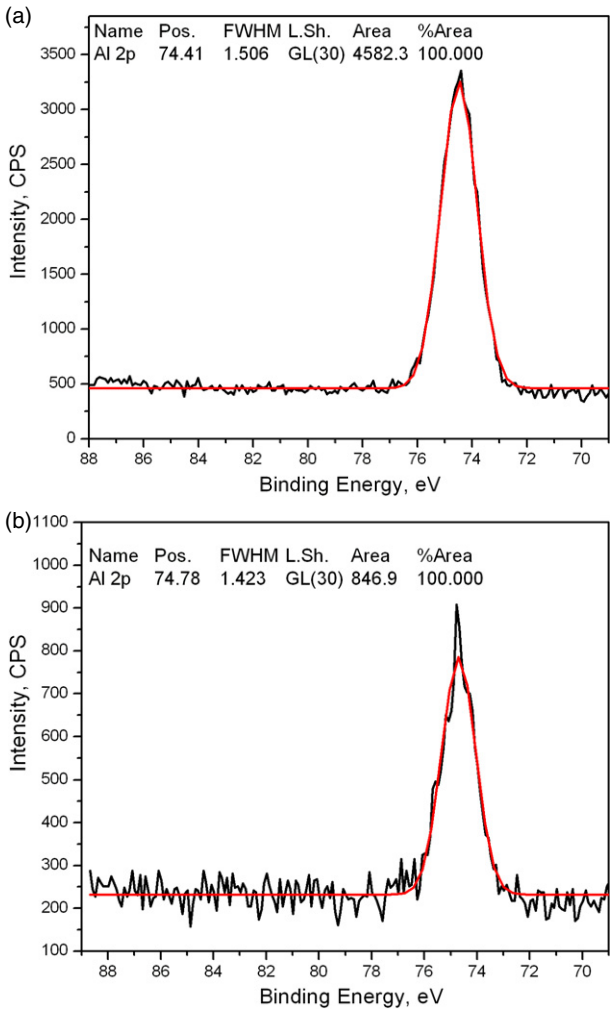

Figure 12. High-resolution XPS spectra of aluminum for the model compound before (a) and after (b) thermal treatment.

aluminum. As shown in figure 10, before treatment, the only chemical environment for nitrogen at 400.01 eV is due to cyanate ester groups, −OCN. After treatment, however, the peak for nitrogen may be deconvoluted into two peaks at 399.65 eV and 400.96 eV, which are assigned to nitrogen in triazine moieties and that in iminocarbonate moieties, respectively [35, 36]. Similarly, it can be seen from figure 11, after the deconvolution, the peak for silicon at 102.80 eV for silicon in silanols or Si–O–Si is also separated out into a new peak at 102.11 eV, which is attributed to the silicon bonding in the iminocarbonate. The study of the silica treated with isocyanate also indicated that the binding energy of silicon was shifted to a lower value, once the hydrogen of the silanols was substituted by iminocarbonate [37]. The authors attributed the shifting to the iminocarbonate groups, which were strong electron-repellent aromatic ester groups. This effect led to a denser electron cloud around the silicon. Consequently the increased shielding effect resulted in the decreased binding energy. Since the aluminols are predominantly located in the inner side and at the ends of the nanotubes, the changed chemical environment for aluminum would not be detectable owing to the wrapping effects as indicated above. As expected, the deconvolution in figure 12 is unsuccessful. The drastically decreased content for the original aluminum (as indicated by the area) is indicative of wrapping of the polymerized cyanate ester on the nanotubes. As suggested by the FTIR and XPS results, it is believed that the silanols and aluminols are reactive towards the cyanate ester and the iminocarbonates are the principal products. The interfacial reactions result in covalently bonded inorganic nanotubes and the matrix, which are responsible for the lowered CTE value, high moduli and morphological characteristics of the hybrids.

4. Conclusion

Naturally occurring HNTs were co-cured with epoxy/cyanate ester resin to form organic–inorganic hybrids. The CTE of the hybrids with low HNT concentration was found to be substantially lower than that of the plain cured resin. For example, the CTE of the hybrids with 12 wt% HNT concentration were found to be 19.6% lower in the temperature range of 25–100 °C and 21.8% lower in the temperature range of 100–160 °C than those for the neat epoxy resin, respectively. The moduli of the hybrids in the glassy state and rubbery state were significantly higher than those for the plain cured resin.

For instance, the glassy and rubbery moduli of the hybrid with 12 wt% HNTs were 58.6% and 121.7% higher than those of the neat epoxy resin, respectively. The dispersion of HNTs in the resin matrix was very uniform. The interfacial reactions took place during the curing of the hybrids between the aluminols and silanols and the cyanate ester. Consequently, the iminocarbonate-bridged interface was formed. The covalently linked interface formed was responsible for the improved performance and morphological characteristics of the hybrids.

Acknowledgment

We are grateful for the financial support by the National Natural Science Foundation of China, grant no. 50603005.

References

[1] Yung K C, Wu J, Yue T M and Xie C S 2006 *J. Compos. Mater.* **40** 567
[2] Yung K C, Wang J and Yue T M 2006 *Adv. Compos. Mater.* **15** 371
[3] Wei Q, Lazzeri A, Di Cuia F, Scalari M and Galoppini E 2004 *Macromol. Chem. Phys.* **205** 2089
[4] Ikegawa N, Hamada H and Yamanouchi M 2002 *Compos. Interfaces* **9** 235
[5] Liu Y X, Kang E T, Neoh K G, Zhang J F, Cui C Q and Lim T B 1999 *IEEE Trans. Adv. Packag.* **22** 214
[6] Konsowski S G and Helland A R 1997 *Electronics Packaging of High Speed Circuitry* (New York: McGraw-Hill)
[7] Sun Y Y, Zhang Z Q and Wong C P 2006 *IEEE T. Compon. Packag. T.* **29** 190
[8] Yang D G, Jansen K M B, Ernst L J, Zhang G Q, Bressers H J L and Janssen J H J 2007 *Microelectron. Reliab.* **47** 233
[9] Ho T H and Wang C S 2001 *Eur. Polym. J.* **37** 267
[10] Teh P L, Mariatti M, Akil H M, Yeoh C K, Seetharamu K N, Wagiman A N R and Beh K S 2007 *Mater. Lett.* **61** 2156
[11] Joussein E, Petit S, Churchman J, Theng B, Righi D and Delvaux B 2005 *Clay Miner.* **40** 383
[12] Tari G, Bobos I, Gomes C S F and Ferreira J M F 1999 *J. Colloid Interface Sci.* **210** 360
[13] Shchukin D G, Sukhorukov G B, Price R R and Lvov Y M 2005 *Small* **1** 510
[14] Du M L, Guo B C, Liu M X and Jia D M 2006 *Polym. J.* **38** 1198
[15] Du M L, Guo B C, Liu M X and Jia D M 2007 *Polym. J.* **39** 2
[16] Liu M X, Guo B C, Du M L and Jia D M 2007 *Appl. Phys.* A **88** 391
[17] Liang K W, Li G Z, Toghiani H, Koo J H and Pittman C U 2006 *Chem. Mater.* **18** 301
[18] Lu X C, Chuan X Y, Wang A P and Kang F Y 2006 *Acta Geol. Sin.-Engl.* **80** 278
[19] Sing K S W, Everett D H, Haul R A W, Moscou L, Pierotti R A, Rouquerol J and Siemieniewska T 1985 *Pure Appl. Chem.* **57** 603
[20] Lu H B, Shen H B, Song Z L, Shing K S, Tao W and Nutt S 2005 *Macromol. Rapid Commun.* **26** 1445
[21] Pinnavaia T J and Beall G W 2000 *Polymer-Clay Nanocomposites* (New York: Wiley)
[22] Yano K, Usuki A and Okada A 1997 *J. Polym. Sci.* A **35** 2289
[23] Luo H X 2006 *Master Thesis* S. China Univ. Technol.
[24] Zheng X G 2005 *Master Thesis* S. China Univ. Technol.
[25] Bauer M, Bauer J, Ruhman R and Kuehn G 1989 *Acta Polym.* **40** 397
[26] Fyfe C A, Niu J, Rettig S J, Wang D W and Poliks M D 1994 *J. Polym. Sci.* A **32** 2203
[27] Martin M D, Ormaetxea M, Harismendy I, Remiro P M and Mondragon I 1999 *Eur. Polym. J.* **35** 57
[28] Guo B C, Fu W W, Jia D M, Qiu Q H and Wang L 2002 *Polym. Polym. Compos.* **10** 237
[29] Frost R L, Kristof J, Mako E and Kloprogge J T 2000 *Am. Mineral.* **85** 1735
[30] Lombardi K C, Guimaraes J L, Mangrich A S, Mattoso N, Abbate M, Schreiner W H and Wypych F 2002 *J. Brazil. Chem. Soc.* **13** 270
[31] Guimaraes J L, Peralta-Zamora P and Wypych F 1998 *J. Colloid Interface Sci.* **206** 281
[32] Farmer V C 1974 *The Infrared Spectra of Minerals* (London: Mineralogical Society)
[33] Farmer V C and Russell J D 1964 *Spectrochim. Acta* **20** 1149
[34] Frost R L 1998 *Clays Clay Miner.* **46** 280
[35] Ripalda J M, de Abajo F J G, Montero I, Galan L and Van Hove M A 2000 *Appl. Phys. Lett.* **77** 3394
[36] Rao W Q, Ren T H, Li J S, Liu W M and Xue Q J 2001 *Tribology* **21** 118 (in Chinese)
[37] Che J F, Xiao Y H, Wang X, Pan A B, Yuan W and Wu X D 2007 *Surf. Coat. Technol.* **201** 4578